

## Experimental and theoretical NEXAFS/XPS study of the room-temperature adsorption of acetonitrile on Si(001)-2×1

S. Rangan, F. Bournel, J.-J. Gallet, S. Kubsky, K. Le Guen, G. Dufour, and F. Rochet\*

Laboratoire de Chimie Physique Matière et Rayonnement, Université Pierre et Marie Curie, 11 rue Pierre et Marie Curie, 75231 Paris Cedex 05, France

F. Sirotti

Laboratoire pour l'Utilisation du Rayonnement Electromagnétique, Centre Universitaire Paris-Sud, Batiment 209D, 91405 Orsay Cedex, France

S. Carniato<sup>†</sup> and V. Ilakovac<sup>‡</sup>

Laboratoire de Chimie Physique Matière et Rayonnement, Université Pierre et Marie Curie, 11 rue Pierre et Marie Curie, 75231 Paris Cedex 05, France

(Received 21 October 2004; revised manuscript received 27 January 2005; published 20 April 2005)

Combining synchrotron radiation N 1s x-ray photoemission and x-ray absorption spectroscopy to density functional theory calculations of electron transition energies and cross sections performed on silicon clusters, we have re-examined the issue of acetonitrile adsorption on single- and two-domain Si(001)-2×1 surfaces, taking into consideration the various adsorption models proposed in the recent theoretical works. It is shown that at 300 K and saturation coverage, the molecule is chemisorbed both under nondissociated and dissociated forms. The nondissociative adsorption mode results from a di- $\sigma$  bonding involving the cyano group. The use of a vicinal surface allows us to show that the *side-on* (a cycloadditionlike product on the Si dimer) is the majority species of di- $\sigma$  type. The datively bonded molecule (*end-on*) is not observed at 300 K. The molecule also dissociates on the surface, under the form of a cyanomethyl *plus* a silicon monohydride, a model which has not been so far proposed by theoretical works.

DOI: 10.1103/PhysRevB.71.165319

PACS number(s): 68.43.Fg, 68.47.Fg, 71.15.Mb, 61.10.Ht

### I. INTRODUCTION

The adsorption of organic molecules on silicon surfaces has developed into a thriving field in current semiconductor research, because of the technological interest in combining the Si-based “infrastructure” with the novel functionalities of an organic “superstructure” (see, for instance, the recent molecular resistivity measurements of Guisinger *et al.*<sup>1</sup>). Nevertheless this field needs some maturation before surface structures with well-defined electronic properties can be exploited. At present, a fundamental research effort has still to be made (i) in the identification of the reaction products—i.e., in the theory-assisted interpretation of spectroscopic data and near-field probe imagery—and (ii) in the understanding of the relevant factors—i.e., kinetics vs thermodynamics—which control the outcome of a surface reaction. The interaction of organics with the “technological” surface, Si(001)-2×1, has been by far the most studied. The dimerized surface (see Fig. 1) is characterized by an asymmetric buckling.<sup>2–4</sup> The asymmetry is associated with an electron transfer between the down atom of the dimer and the up atom. Chemically, this means that the up atom can act as a Lewis base, while the down atom acts as a Lewis acid. Anchoring units leading to nondissociative molecular grafting on the clean surface have already been identified. They have been essentially  $\pi$ -bonded units, vinyl and acetylenic moieties, that bind on the surface by opening a  $\pi$  bond and forming two strong  $\sigma$  Si-C bonds with a pair of silicon dangling bonds.<sup>5</sup> On the dimer (site A), the reaction intermediate

is thought to be a low symmetry state, donating its  $\pi$  electrons to the acidic silicon site.<sup>6,7</sup>

The cyano (-C $\equiv$ N:) functional group, being isoelectronic to (-C $\equiv$ C-), is another potential anchoring unit for grafting organics on Si. In that respect, acetonitrile (CH<sub>3</sub>C $\equiv$ N:) appears at first glance as a model system. Taking into consideration a *sp*-to-*sp*<sup>2</sup> rehybridization scheme, di- $\sigma$  bonding geometries (Si-C $\equiv$ N-Si) can result from the reaction of the  $\pi$  system with the surface. The first one, the *side-on* geometry that can form on a silicon dimer (site A of Fig. 1) is sketched in Fig. 2(a). Alternately the molecule could bridge two Si dangling bonds across two adjacent

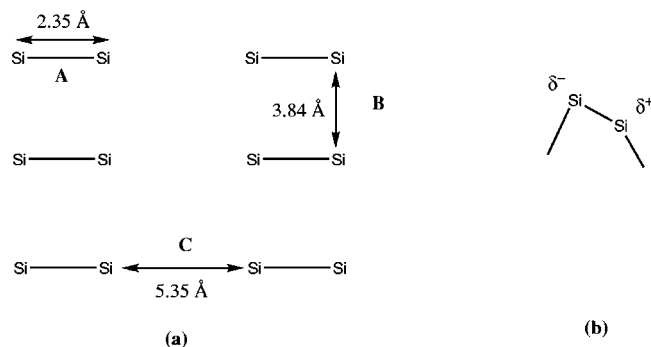


FIG. 1. (a) The 2×1 reconstructed surface and three adsorption sites. (b) The asymmetry of the dimers is associated to a charge transfer between down and up silicons.

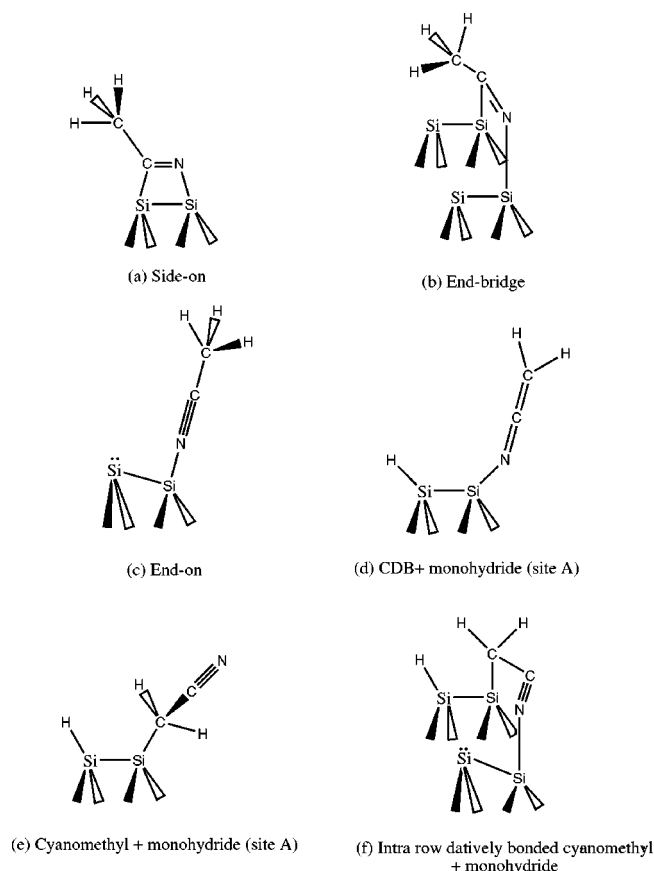


FIG. 2. Possible adsorption modes of acetonitrile adsorbed on Si(001)- $2 \times 1$ .

dimers of the same row (site *B* of Fig. 1), to give an *end-bridge* geometry [Fig. 2(b)].

Yet, besides di- $\sigma$  bonding on Si via  $\pi$  bond opening, other bonding possibilities must be envisaged. First the nitrogen lone pair, can be involved in a dative bond with the acidic Si site in an *end-on* configuration [Fig. 2(c)]. Second, the acidic nature of the  $\alpha$ H atom has to be taken into account,<sup>8</sup> and dissociated geometries have to be envisaged. A  $\alpha$ H could be transferred to a silicon dangling bond while the  $\text{CH}_2\text{CN}$  moiety could bind to a second silicon dangling bond, to give

either a  $\text{Si-N}=\text{C}=\text{CH}_2$  *cumulative-double-bond* (CDB) unit or a  $\text{Si-CH}_2\text{-C}\equiv\text{N}$  *cyanomethyl* unit. For instance, on site *A*, the CDB and cyanomethyl (plus silicon monohydride) geometries are depicted in Figs. 2(d) and 2(e), respectively. Given that a cyanomethyl can rotate around its Si- $\alpha$ C axis, its nitrogen ending could also make a dative bond with dangling bonds of neighboring silicon dimers (site *B* and *C* of Fig. 1). The intrarow *datively bonded cyanomethyl* is depicted in Fig. 2(f).

Feng Tao and co-workers,<sup>9</sup> made the first experimental study of the adsorption of acetonitrile on Si(001)- $2 \times 1$  (at 110 K), using high resolution electron energy loss spectroscopy (HREELS). After annealing at 300 K, they observed a peak at  $1603 \text{ cm}^{-1}$  (197 meV), attributed to the stretching mode of a  $sp^2$  rehybridized adspecies ( $\text{C}=\text{N}$ ). Moreover a characteristic methyl bending mode was also detected. Therefore the side-on or end-bridge geometries, are likely products. These authors also observed that the signature characteristic of an end-on geometry (i.e., a  $\text{C}\equiv\text{N}$  stretching mode) was absent after room temperature annealing, pointing to the fact that the end-on cannot be stabilized at 300 K.

In a subsequent experimental work, our group used synchrotron radiation spectroscopies [N  $1s$  x-ray photoemission spectroscopy (XPS) and N  $1s$  near-edge x-ray absorption fine structure spectroscopy (NEXAFS)] to examine the products resulting from the reaction of acetonitrile with Si(001) at 300 K.<sup>10</sup> We detected multiple hybridization states for the CN group, in contrast to the findings of Feng Tao *et al.*,<sup>9</sup> who observed only  $\text{C}=\text{N}$  products after a 110 K adsorption/300 K annealing. The two main  $\pi^*$  transitions we observed were tentatively attributed (i) to a Si-C=N-Si unit (having its  $\pi$  system contained in the surface plane) and (ii) to a  $\text{C}\equiv\text{N}$  moiety (which did not give rise to pronounced x-ray absorption dichroism). We concluded that the latter product could result from the dissociation of the molecule, without specifying its nature, or from a N lone pair dative bond.

The experimental works have stimulated theoretical calculations of the adsorption energetics of  $\text{CH}_3\text{CN}$  on Si(001) using the density functional theory (DFT) approach.<sup>11-13</sup> Adsorption energies from the literature are collected in Table I.

Cho and Kleinman<sup>11</sup> have restricted their analysis to non-dissociative cases. Using DFT and modelling the surface by

TABLE I. DFT adsorption energies reported in the literature, “Cho” from Ref. 11, “Mui” from Ref. 12, “Miotto” from Ref. 13. Periodic slab geometries are calculated for a molecular coverage of 0.5 monolayer. Adsorption energies that are obtained as by-products of our DFT calculations (see Sec. III A), are also included for comparison.

| Geometry         | DFT adsorption energies (eV) |                          |                                    |                    |
|------------------|------------------------------|--------------------------|------------------------------------|--------------------|
|                  | Periodic slab                |                          | $\text{Si}_9\text{H}_{12}$ cluster |                    |
|                  | Cho                          | Miotto                   | Mui                                | This work          |
| End-on           | -0.91/0.00 <sup>a</sup>      | -0.91/0.00 <sup>a</sup>  | -0.61/0.00 <sup>a</sup>            | 0.00 <sup>a</sup>  |
| Side-on          | -1.47/-0.56 <sup>a</sup>     | -1.60/-0.69 <sup>a</sup> | -1.09/-0.48 <sup>a</sup>           | -0.54 <sup>a</sup> |
| End-bridge       | -1.43/-0.52 <sup>a</sup>     | -1.28/-0.37 <sup>a</sup> |                                    |                    |
| CDB              |                              |                          | -1.54/-0.93 <sup>a</sup>           | -0.80 <sup>a</sup> |
| Free Cyanomethyl |                              |                          |                                    | -1.18 <sup>a</sup> |

<sup>a</sup>Relative to the adsorption energy of the end-on model.

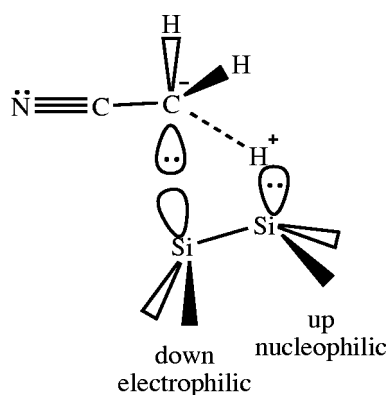


FIG. 3. A possible reaction path leading to the formation of a cyanomethyl plus monohydride.

a periodic slab geometry (a  $2 \times 2$  unit cell), they found that the *side-on* (respectively, paired *end-bridge*) configuration is the more stable, at 0.5 (respectively, 1) monolayer coverage, a situation similar to the acetylene case.<sup>14</sup> Cho and Kleinman have calculated the reaction paths of both products from an end-on precursor: an activation barrier of 0.26 eV (respectively,  $\sim 0$  eV) is found for the side-on (respectively, end bridge). Therefore the end-bridge product should be kinetically favored, at least at low coverage.

In their DFT cluster calculations, Mui *et al.*<sup>12</sup> have examined the formation of the side-on adduct (*via* an end-on precursor), but they have also taken into consideration the issue of molecular dissociation. They have calculated the formation of a CDB [Fig. 2(d)] formed from the end-on precursor, and found it 0.44 eV more stable than the side-on (the calculated activation barrier is only 0.04 eV larger than that of the end-on to side-on transformation).

Note that the two theoretical works cited in Refs. 11 and 12 share the common view that the precursor to molecular adsorption and/or dissociation is the end-on adduct. For instance the CDB could result from an end-on intermediate which bends to transfer a proton to the nucleophilic up dimer atom.<sup>12</sup> Alternately, another H transfer mechanism, leading to cyanomethyl grafting, can be imagined as depicted in Fig. 3. The nucleophilic up dimer atom harpoons a proton, leaving a  $\text{CH}_2\text{CN}^-$  anion. The  $\alpha$  carbon, which now bears a “formal” lone pair—calculations<sup>15</sup> show indeed that the pyramidalization angle ( $\angle\text{CCH}$ ) at the carbonion carbon is in the range  $114^\circ$ – $115.7^\circ$ —makes a dative bond with the electrophilic down dimer atom, resulting in a Si- $\text{CH}_2\text{CN}$  moiety.

Very recently, Miotto and co-workers<sup>13</sup> have made periodic DFT calculation, supporting the existence of the side-on on the surface. They have also found that the end-on model is also possible. In contrast to the preceding theoretical works,<sup>11,12</sup> Miotto and co-workers do not find that the end-on is a precursor to the side-on, as any distortion of the end-on leads to its desorption.

The goal of the present study is the determination of the adsorption geometries of acetonitrile at room temperature on Si(001), by combining radiation synchrotron electron spectroscopy data and electron transition energy computation. At the experimental level, we have used N 1s photoemission and NEXAFS spectroscopy, which inform on the nature of

the chemical bonding. *K*-edge NEXAFS is a powerful synchrotron radiation technique which probes the unfilled states of *p* symmetry. It is able to detect the presence of specific bonds in the molecules (e.g.,  $\pi$  bonds via the observation of a  $1s \rightarrow \pi^*$  resonance at a photon energy close to the N 1s binding energy). NEXAFS gives also information on the orientation of the unoccupied *p* orbitals. The dipole absorption from a  $1s$  level has a characteristic  $\cos^2(\delta)$  dependence, where  $\delta$  is the angle between the *p* orbital axis and the polarization vector *E* of the synchrotron radiation.<sup>16</sup> Therefore bond directions can be inferred from the experimental dichroic absorption spectra, and adsorption models can be readily eliminated.

Yet, our philosophy was to go beyond such a straightforward interpretation of the experimental data. As a matter of fact the systematic calculation of NEXAFS spectra is highly desirable in modern synchrotron radiation spectroscopy applied to surface science, as far as only the knowledge of the energetics (x-ray absorption transition energies and ionization potentials) would permit a rigorous attribution of the experimental lines to any particular model. However, because many different chemisorbed forms of the molecule on the substrate can exist, it is crucial to numerically resolve with high precision both the energy position and the intensity of the resonances corresponding to the various species.

In this context, DFT seems to be the most suitable approach. It can take into account both relaxation and correlation effects at a moderate computational cost. It has been shown that the  $\Delta\text{SCF}$  type of approach can be adopted for the DFT Kohn-Sham orbital theory, i.e., the “ $\Delta$  Kohn-Sham” method as proposed by Triguero *et al.*,<sup>17</sup> in which ionization potentials and transition energies are obtained through separately optimized ground and excited states. Like for Hartree-Fock (HF) based methods the “ $\Delta\text{KS}$ ” method improves reaching experimental agreement within a few tenths of an eV as recently shown in Refs. 17 and 18 for isolated molecules. In the present paper we apply this kind of approach to the case of molecular adsorbates grafted on a semiconductor surface, Si(001)- $2 \times 1$ , that we simulate by clusters of various sizes.

## II. EXPERIMENT

### A. Sample preparation

#### 1. Si cleaning

Si samples are cut into phosphorus doped wafers, of resistivity  $0.003 \Omega \text{ cm}$ . They are cleaned from their native oxide by flashing at  $1250^\circ\text{C}$ . The surface reconstructions are checked by low energy electron diffraction (LEED).

#### 2. Single domain Si(001) surfaces

To take a full advantage of the capability of N 1s NEXAFS spectroscopy to determine bond orientations, the acetonitrile molecule needs to be deposited on a single-domain vicinal surface. It is well known that on-axis [nominal (001)] surfaces consist of  $2 \times 1$  and  $1 \times 2$  domains in equal quantities, with the dimer rows of one domain running perpendicular to the dimer rows of the other. On the other hand, a

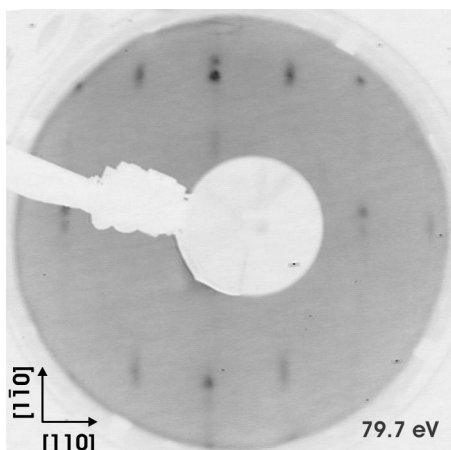


FIG. 4. LEED pattern of a Si(001)- $2 \times 1$  vicinal surface, saturated with acetonitrile. The step edge is along the [110] direction. The energy of the electron beam is 79.7 eV.

vicinal Si(001) surface, cut by more than  $2^\circ$  off [001] axis, toward  $[1\bar{1}0]$ , forms a regular array of bi-steps and single  $2 \times 1$  reconstructed surface domain terraces. Here the surface is misaligned by  $5^\circ$ . We have checked by LEED that a single-domain pattern is observed. We give in Fig. 4 the LEED image of a vicinal surface saturated with acetonitrile. Note that half-order spots are only seen along the [110] direction. Spot doubling along the  $[1\bar{1}0]$  direction reflects the step edge periodicity of terraces with equal widths.

### 3. Acetonitrile dosing

Acetonitrile is a commercial product (Aldrich), purified by several freeze-pump-thaw cycles. It is dosed onto the silicon surface cooled at room temperature, through a leak-valve under constant pressure in the  $10^{-8}$ – $10^{-7}$  mbar range (the gauge reading being uncorrected) for 600 s, in order to achieve the saturation coverage. The gas cleanliness is checked with a mass quadrupole analyzer.

## B. Electron spectroscopies

### 1. Synchrotron radiation

The experiments have been performed at Beamline SB7/ experimental station ABS6 of LURE-Super ACO synchrotron facility (Orsay, France). The photon energy is calibrated using the difference in energy of both, first and second order light from the Dragon-type monochromator. The source being a bending magnet, the degree of linear polarization is 95%. The larger component of the electric field ( $E$ ), lies in the horizontal orbital plane of the storage ring. The Auger yield (AY) mode has been used to increase the adsorbate-to-Si bulk signal ratio. A Scienta 200 hemispherical electron analyzer, working in fixed mode, is used for that purpose: 18 eV wide energy windows, centered at 363, 373, and 383 eV were chosen. To obtain reasonable count rates the photon band width was around 180 meV. Angle dependent measurements have been carried out. The sample was mounted on a vertical sample holder, so that the polar angle  $\theta$  between  $E$

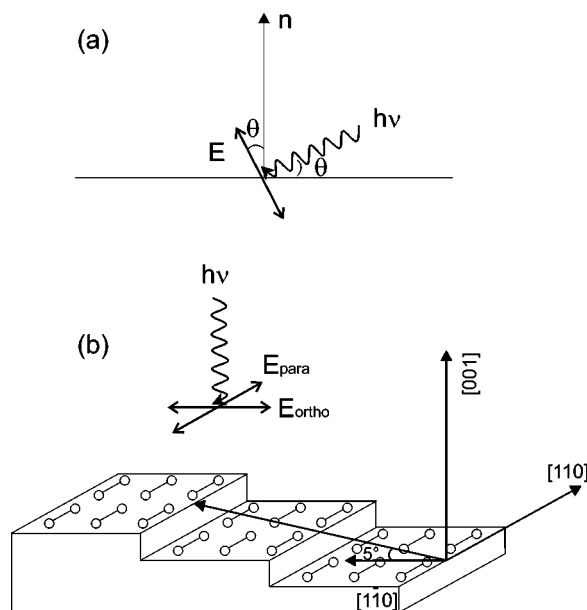


FIG. 5. (a) For a photon incidence of  $\theta$  relative to the surface plane, the electric field makes an angle  $\theta$  with respect to the normal ( $n$ ) to the surface. (b) In normal incidence on a vicinal surface the electric field can be parallel ( $E_{\text{para}}$ ) or orthogonal ( $E_{\text{ortho}}$ ) to the dimer axis. The crystallographic directions are indicated.

and the surface normal can be changed between  $\theta=90^\circ$  (normal incidence) and  $\theta=16^\circ$  (grazing incidence). The azimuthal orientation of  $E$  with respect to the surface crystallographic directions can also be modified by rotating the sample around the normal to its surface. In the case of a single-domain Si(001) surface, under normal incidence ( $\theta=90^\circ$ )  $E$  can be placed either parallel or perpendicular to the axis of a “symmetric”  $\text{Si}_2$  dimer, as depicted in Fig. 5.

### 2. Photoemission

Core-level (Si  $2p$ , C  $1s$ , N  $1s$ ) photoemission spectra were also recorded with the hemispherical analyzer working in swept mode. Binding energies are measured with respect to the Fermi level (FL). Additional valence band spectra were also measured using a He I lamp as an excitation source.

## III. COMPUTATIONAL

### A. Geometry optimization

Electronic structure calculations were completed with the GAMESS(US) (Ref. 19) software package using Becke3 Lee-Yang-Parr (B3LYP) three parameter DFT theory. Geometries of local minima on the potential energy surface were calculated with a  $6-311G^*$  basis set for nitrogen, carbon and silicon atoms. The H ligands are described by a  $6-31G^*$  basis. When the adsorption site involves only one dimer [as in models (a), (c)–(e) of Fig. 2], the Si(001)- $2 \times 1$  surface is modelled with a  $\text{Si}_9\text{H}_{12}$  cluster. The top two silicon atoms compose the surface dimer, while the remaining seven Si atoms, compose three subsurface layers which are hydrogen terminated to preserve the  $sp^3$  hybridization of the bulk diamond lattice. Using the  $\text{Si}_9\text{H}_{12}$  cluster, adsorption energies—

relative to that of the end-on model, see Table I—are in good accord with those previously calculated with a cluster of the same size.<sup>12</sup> When the adsorption involves two dimer sites pertaining to the same row [as in models (b) and (f) of Fig. 2] a  $\text{Si}_{15}\text{H}_{16}$  cluster was used.

It has been shown that the cluster size has some effect on molecule-to-silicon charge transfers, and therefore on the calculated adsorption heat, for instance, Widjaja *et al.*<sup>20</sup> have shown that the  $\text{Si}_{21}\text{H}_{20}$  three-dimer cluster is necessary and adequate to describe the dative adsorption of *one*  $\text{NH}_3$  molecule on  $\text{Si}(001)$ . (Note that the many-dimer large clusters are intended to address the low coverage limit.) One could wonder if the cluster size could also affect considerably the calculated excited state energies of the adsorbed molecule. To our knowledge, DFT works dealing explicitly with this effect in the case of molecules on semiconductors have not been published yet. The reason may be purely “technical,” as the convergence of the excited states may be difficult for very large clusters (see below, Sec. III B). Note that the “small”  $\text{Si}_9\text{H}_{12}$  cluster representing a single-dimer site has been recently used in a DFT calculation of the x-ray emission spectrum for ethylene adsorbed on  $\text{Si}(001)$ .<sup>21</sup> However to examine this size issue, the end-on bonding has been taken as a test case. The possible influence of charge delocalization along a dimer row (see Ref. 20) on the N  $1s$  transition energies is examined using a cluster comprising three dimers in the same row ( $\text{Si}_{21}\text{H}_{20}$ ), placing the molecule on the central dimer, leaving the other two free. In addition to the three-dimers-in-a-row cluster, we have also used a double-dimer cluster ( $\text{Si}_{23}\text{H}_{24}$ ) to study the effect of increasing the cluster size across the trench separating the dimer rows.

### B. N $1s$ NEXAFS calculations

The local minima geometries we find for the molecule plus Si cluster system are the starting point of the calculation of NEXAFS transitions and ionization potentials (IP). The quantum chemical *ab initio* calculations of excited states are performed at a DFT level of theory. The application of DFT to core-photoionization phenomena takes advantage that both the relaxation and correlation effects are simultaneously described at a moderate computational cost, with respect to SCF and post-HF methods. We used a modified version of the GAMESS(US) program, enabling (i) the choice of a fractional occupancy for the core hole and (ii) the calculation of singlet core excited energy values.<sup>18</sup> We used an IGLOO-III basis set<sup>22</sup> for the nitrogen atom along with a special diffuse [ $3s, 3p, 3d$ ] added at the core ionized/excited site.

One of the main problems encountered in the present simulation was the SCF convergence of core excited states within a large system, that is, the adduct and the silicon cluster representing the surface. The large basis sets indicated above are necessary (i) to describe correctly the drastic changes in the electronic structure in the vicinity of the core excited or ionized site, and (ii) to represent properly the Rydberg transitions near the photoionization edge. Not only is the computation procedure relatively time consuming, but the convergence of the core excited final states may be difficult to reach, especially for large systems. To overcome this

difficulty, we have introduced a procedure which consists in optimizing decreasing fractional occupancies for the core electron (between 1 and 0). Generally, no convergence problems are encountered for the small silicon cluster ( $\text{Si}_9\text{H}_{12}$ ). However for larger clusters, such as the triple-dimer cluster ( $\text{Si}_{21}\text{H}_{20}$ ), the convergence process may be rather tedious, especially for singlet DFT core excited states (see below).

The variational principle can be applied to densities referring to any state with fractional occupancy. The NEXAFS spectra are calculated in the framework of the transition potential (TP) method, in which relaxation effects are treated by second order perturbation theory, the DFT calculation optimizes the ionic state corresponding to a fractional electron occupancy of the  $1s$  orbital equal to 1.5. Then transition energies are obtained as the difference between the energies of the virtual orbital and that of the  $1s$  orbital. X-ray absorption cross sections are calculated by use of the mono-electronic core and excited-state TP virtual orbitals within the dipolar approximation. (It is assumed that the radiation is linearly polarized.)

The TP method gives accurate relative NEXAFS transition energies (see below) but absolute values are typically 0.5–1 eV off the experimental ones. Therefore NEXAFS spectra are repositioned on an absolute energy scale by a DFT calculation of the first (lower  $h\nu$ ) bound excited state, for which one electron is removed from the  $1s$  and one is added to the empty orbital of interest. Then the transition energy is obtained as the difference between the energies of the excited state and of the ground state (in the following this “ $\Delta$  Kohn-Sham” method is denoted  $\Delta\text{KS}$ ). The relativistic correction of 0.3 eV is included, according to Triguero *et al.*<sup>17</sup> The  $\Delta\text{KS}$  triplet final state transition energies are corrected using the sum method of Ziegler, Rauk, and Baerends<sup>23</sup> in order to account for the spin conservation in dipolar transitions leading to a singlet final state. This leads to transition energies fairly close to experimental ones, as tested for free molecules.<sup>18</sup>

For the calculation of N  $1s$  ionization potentials (IP), the same  $\Delta\text{KS}$  method is applied, IP being the difference between the energy of the excited state, represented by a core hole in the N  $1s$  orbital, and that of the ground state.

Steplike features, referred as “continuum steps,”<sup>24</sup> are observed in the experimental NEXAFS spectra. Steps are the result of excitation of the core electron to a (quasi) continuum of final states. In isolated molecules, the step occurs at the IP, due to the transition to the free-electron continuum. We have considered that the adspecies plus Si cluster can be considered as a molecule, having discrete bound states below IP and discrete states *embedded in the energy continuum of the free electron above IP*. Below IP, the NEXAFS spectrum consists of the DFT-TP calculated lines broadened by convolution with a Gaussian of 0.6 eV full-width at half-maximum (FWHM). Above IP, to describe the continuum part of the spectrum, the DFT-TP method is connected to the Stieltjes imaging procedure,<sup>25</sup> which converts the “above-IP” discrete lines into a continuum (the calculated continuum cross section is convoluted with the same Gaussian function used for the discrete part below IP).

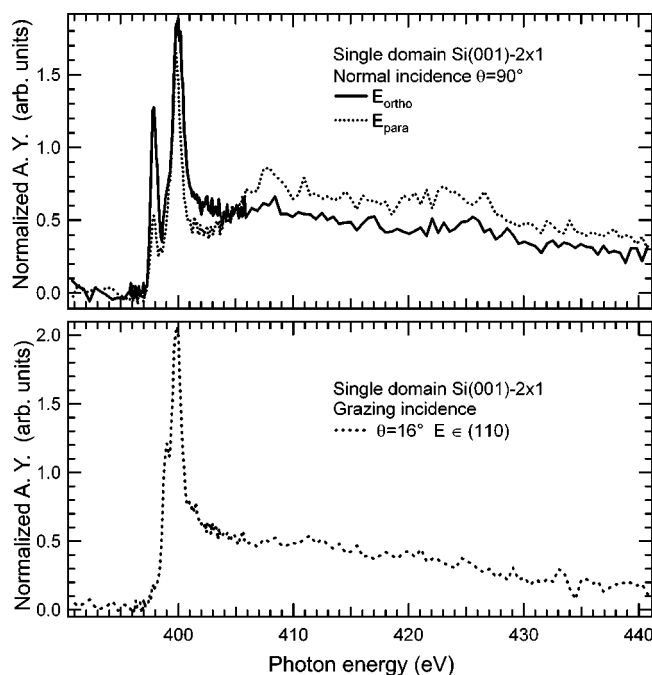


FIG. 6. Normalized N 1s NEXAFS spectra of the single-domain Si(001)-2 $\times$ 1 surface exposed to acetonitrile under a pressure of  $10^{-7}$  mbar for 600 s. (a) Normal incidence. (b) Grazing incidence. The dimer rows run in a [110] direction (see also Fig. 5). Peak assignments are reported in Table IV.

#### IV. N 1s NEXAFS AND XPS EXPERIMENTAL DATA

The exposure of the silicon (001) surfaces to acetonitrile (under a pressure of  $10^{-7}$  mbar, for 600 s, at a temperature of 300 K) corresponds to a situation in which all silicon surface states are consumed, as checked by He I valence band photoemission (not shown). The Si  $2p_{3/2}$  level move by 0.15 eV to higher binding energy with respect to the clean surface position, in relation to a change in band curvature at the surface. The N 1s NEXAFS spectra of chemisorbed layers are given in Fig. 6, for a single-domain Si(001)-2 $\times$ 1 surface, and in Fig. 7 for a “nominally flat” two-domain surface.

Three bound resonances (at photon energies 397.8 eV, 399.0 eV, and 399.8 eV) and one continuum resonance (“ $\sigma^*$ ”-like, at a photon energy of  $\sim$ 408 eV) are observed in the NEXAFS spectra of the single- and two-domain surface, showing that no detectable extra adspecies are present on the single-domain surface, because of its high step density. Grazing incidence spectra, for which  $E$  is nearly perpendicular to the surface are nearly identical. The normal incidence spectrum of the two-domain surface can be reconstituted by summing the two normal incidence spectra of the single-domain surface, taken with  $E$  parallel to the dimer axis or perpendicular to them. This means that the products formed on single- and two-domain surfaces give identical NEXAFS signature, and that their relative distribution is nearly the same. First let us focus on the  $\pi^*$  (397.8 eV) and  $\sigma^*$  (408 eV) resonances which are polarized in the surface plane. When using a single-domain surface, a strong in-plane azimuthal dichroism in normal incidence can be noticed in Fig. 6 for this  $\pi^*$  resonance when  $E$  changes from a direction orthogo-

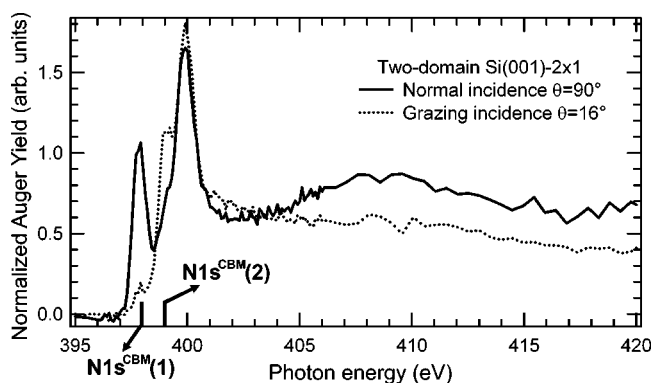


FIG. 7. Normalized N 1s NEXAFS spectra of the two-domain Si(001)-2 $\times$ 1 surface exposed to acetonitrile under a pressure of  $10^{-7}$  mbar for 600 s at a temperature of 300 K. The binding energies (relative to the conduction band minimum) of the two XPS spectral lines (Fig. 8) are indicated with vertical bars [ $N 1s^{CBM}(1)$  and  $N 1s^{CBM}(2)$ ]. Peak assignments are reported in Table IV.

nal to the dimer axis ( $E_{ortho}$ , the Auger yield intensity is maximum,  $I=I_{max}$  (see also Fig. 5) to a direction parallel to the dimer axis ( $E_{para}$ , the Auger yield is minimum, and equal to  $I_{max}/3$ ). For its part, the  $\sigma^*$  transition appears polarized at right angle with respect to the  $\pi^*$  resonance, being maximum (minimum) for  $E_{para}$  ( $E_{ortho}$ ).

The second bound transition observed at 399.0 eV (Figs. 6 and 7), is better seen at grazing incidence. Its position coincides with a continuum step, related to the onset of transitions to silicon states mixed with molecular levels.<sup>24</sup>

The third bound transition is observed at 399.8 eV (Figs. 6 and 7). It appears weakly dichroic both for single-domain and two-domain surfaces. We will limit ourselves to noting that this transition energy is close to that of a free acetonitrile molecule ( $399.9 \pm 0.1$  eV).<sup>26</sup>

The N 1s XPS spectrum of a two-domain Si(001) surface (saturation coverage) is given in Fig. 8.

Two spectral lines are found at binding energies (referred to the Fermi level) 397.8 [ $N 1s^{FL}(1)$ ] and 398.7 eV [ $N 1s^{FL}(2)$ ], respectively. Therefore XPS points to (at least)

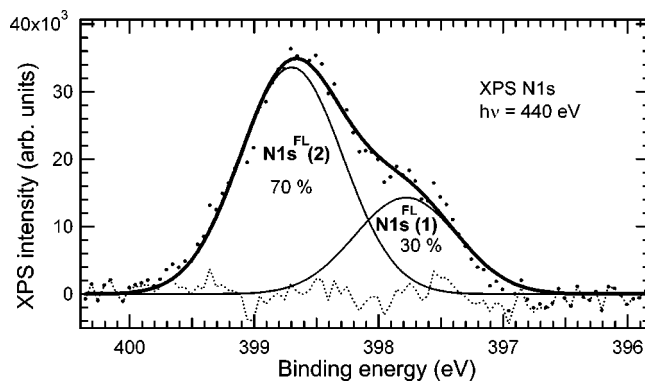


FIG. 8. N 1s photoemission spectrum (dots) of a two-domain Si(001) surface exposed to acetonitrile at 300 K (saturation coverage). The binding energy is measured with respect to the Fermi level. A best fit (solid curves) is also given, the FWHM of each spectral line is 0.97 eV. Peak assignments are reported in Table IV.

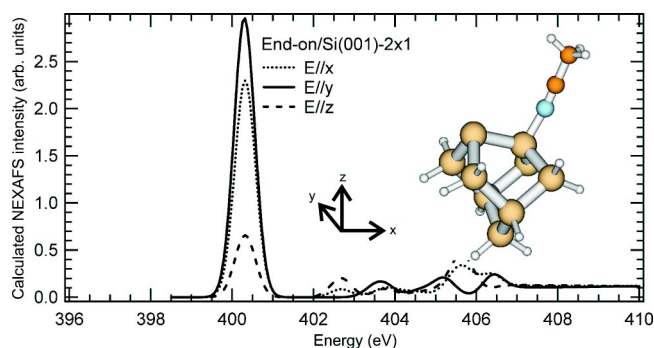


FIG. 9. (Color online) Calculated NEXAFS spectra of the end-on model, for three directions of the electric field. The optimized geometries are given in the inset.

the presence of two species. The measured  $[N 1s^{FL} (1)]:[N 1s^{FL} (2)]$  intensity ratio is 30:70.

## V. INTERPRETATION

### A. Calculated N 1s NEXAFS spectra

#### 1. The isolated molecule

For the isolated molecule, we obtain a calculated IP of 405.6 eV and a calculated NEXAFS  $\pi_{C\equiv N}^*$  transition of 399.9 eV. Therefore the  $\Delta$ KS calculations are in excellent agreement with the experimental IP [405.6 eV (Ref. 27)] and  $1s \rightarrow \pi^*$  transition energies  $[399.9 \pm 0.1$  eV (Ref. 26)] of the molecule in the gas phase.

#### 2. The end-on model

In the end-on model the molecule is datively bonded to a silicon dangling bond. In a Lewis picture, the “free” dangling bond is occupied by two electrons, forming a lone pair. Therefore a buckling is expected, the lone pair bearing silicon moving up, and the molecule-bearing silicon moving down (see, e.g., the triethylamine case<sup>28,29</sup>). This situation is specific to the end-on geometry. For all the other geometries studied here (side-on, Si-H plus CDB, Si-H plus cyanomethyl), no dangling bonds are left on the dimer site, and buckling is weak or absent.

The optimized geometry is depicted in the inset of Fig. 9 for a calculation performed on a single-dimer cluster ( $Si_9H_{12}$ ). Geometrical outputs are reported in Table II. The molecule datively bonded to a silicon atom conserves a CN bond-length characteristic of a triple bond (1.15 Å). The CN axis makes an angle of  $11^\circ$  with respect to the normal to the surface: the  $\pi$  bond system is therefore nearly parallel to the surface. As expected, the calculated NEXAFS spectrum exhibits a  $\pi_{C\equiv N}^*$  transition (at  $h\nu=400.3$  eV) strongly polarized in the  $xy$  plane [Fig. 9]. The IP is calculated at 406.72 eV.

For this particular adsorption mode, we have examined the influence of the cluster size on the transition energies. The transition energies for the three clusters are collected in Table III. Using the three-dimers-in-a-row cluster,  $Si_{21}H_{20}$ , the NEXAFS  $\pi_{C\equiv N}^*$  transition is calculated at an energy of 400.3 eV, equal to that calculated for the  $Si_9H_{12}$  cluster. On the other hand the IP is calculated at 406.37 eV, slightly shifted down (by 0.35 eV) with respect to that obtained in the single-dimer calculation. Using the other large cluster, the trench (double-dimer) cluster  $Si_{23}H_{24}$ , we find NEXAFS and IP energies equal to those calculated for the  $Si_{21}H_{20}$  one.

We note that the effect of an increasing cluster size on the N 1s NEXAFS transition energy is almost negligible, while the IP decreases by a few tens of eV. The comparison of the two large clusters and is also of interest. As indicated in Ref. 20 for the related case of  $NH_3$  datively bonded to a silicon dimer, charge delocalization is greater for the three-dimers-in-a-row cluster ( $Si_{21}H_{20}$ ) than for the trench (two-dimer) cluster ( $Si_{23}H_{24}$ ). This means that two adjacent dimer rows are nearly independent. Therefore, initial state IP shifts, relative to the single-dimer cluster, should be larger for the  $Si_{21}H_{20}$  cluster than for the  $Si_{23}H_{24}$  one. As the two calculated IPs are nearly identical, it seems reasonable to assume that initial state effects (as a function of the cluster size) are small. Thus the trend observed for the IP (a decrease with increasing cluster size) could be related to a better screening of the nitrogen core hole when the number of Si atoms surrounding it increases. On the other hand, the NEXAFS peak position would remain largely unaffected by the silicon

TABLE II. Calculated distances and angles of the optimized geometries. Distances are given in Å and angles in degrees. The  $xy$  plane corresponds to the surface plane and the  $z$  direction to the surface normal.  $y$  is perpendicular to the dimer axis. Calculations are performed with a single-dimer cluster  $Si_9H_{12}$ , except for the dative cyanomethyl, for which a two-dimers-in-a-row cluster ( $Si_{15}H_{16}$ ) is used.

|                | End-on | Side-on | CDB   | Cyanomethyl | Dative cyanomethyl |
|----------------|--------|---------|-------|-------------|--------------------|
| $d_{Si-Si}$    | 2.39   | 2.35    | 2.41  | 2.40        | 2.38(N)/2.39(C)    |
| $d_{C-N}$      | 1.15   | 1.29    | 1.21  | 1.15        | 1.16               |
| $d_{C-C}$      | 1.45   | 1.50    | 1.31  | 1.45        | 1.42               |
| $d_{Si-C}$     |        | 1.98    |       | 1.94        | 2.03               |
| $d_{Si-N}$     | 1.91   | 1.83    | 1.77  |             | 2.00               |
| $d_{C-H}$      | 1.09   | 1.09    | 1.08  | 1.09        | 1.09               |
| $\angle CCN$   | 179.5  | 122.2   | 177.2 | 177.5       | 165.1              |
| $\angle SiNC$  | 172.8  | 103.1   | 135.5 |             | 125.4              |
| $\angle SiSiN$ | 107.9  | 79.2    | 118.1 |             | 106.7              |
| $\angle HCH$   | 109.3  | 109.7   | 119.2 | 107.6       | 110.4              |

TABLE III. Calculated  $\Delta$ KS NEXAFS transitions

| Model                    | Calculated NEXAFS transitions | Type polarization                                 | Calculated IP |
|--------------------------|-------------------------------|---|---------------|
| Free molecule            | 399.9                         | $\pi_{\text{C}\equiv\text{N}}^*$                  | 405.6         |
| End-on <sup>b</sup>      | 400.3                         | $\pi_{\text{C}\equiv\text{N}}^*E//\mathbf{xy}$    | 406.72        |
| End-on <sup>c</sup>      | 400.3                         |   | 406.37        |
| End-on <sup>d</sup>      | 400.3                         |   | 406.36        |
| Side-on <sup>b</sup>     | 398.0                         | $\pi_{\text{C}\equiv\text{N}}^*E//\mathbf{y}$     | 403.3         |
|                          | 398.8 <sup>a</sup>            | $\sigma_{\text{Si-N}}^*E//\mathbf{z}$             |               |
| CDB <sup>b</sup>         | 399.3                         | $\pi_{\text{C}=\text{C}=\text{N}}^*E//\mathbf{y}$ | 404.5         |
|                          | 402.2 <sup>a</sup>            | $\pi_{\text{C}=\text{C}=\text{N}}^*E//\mathbf{x}$ |               |
| Free                     | 399.7                         | $\pi_{\text{C}\equiv\text{N}}^*$                  | 404.7         |
| cyanomethyl <sup>b</sup> |                               |   |               |
| Intrarow                 | 399.6                         | $\pi_{\text{C}\equiv\text{N}}^*E//\mathbf{z}$     | 405.7         |
| Cyanomethyl <sup>c</sup> | 400.2 <sup>a</sup>            | $\pi_{\text{C}\equiv\text{N}}^*E//\mathbf{x}$     |               |

<sup>a</sup>Calculated by adding the TP model energy shift to the absolute  $\Delta$ KS value of the lower energy transition) and  $\Delta$ KS IPs for various models of the acetonitrile/Si(001) system.

<sup>b</sup>Si<sub>9</sub>H<sub>12</sub> single-dimer cluster.

<sup>c</sup>Si<sub>21</sub>H<sub>20</sub> three-dimers-in-a-row cluster.

<sup>d</sup>Si<sub>23</sub>H<sub>24</sub> trench (double-dimer) cluster.

<sup>e</sup>Si<sub>15</sub>H<sub>16</sub> two-dimers-in-a-row cluster. Energies are given in eV.

cluster size as the core hole is screened by the electron promoted in the  $\pi^*$  orbital. The same cluster size effects are obtained in the case of benzonitrile grafted to a silicon dimer via a Si-C=N-Si unit.<sup>30</sup> In the latter case, the N 1s NEXAFS transition is not affected by an increase in the cluster size (from a Si<sub>9</sub>H<sub>12</sub> cluster to a Si<sub>21</sub>H<sub>20</sub> cluster), while the IP decreases by about 0.25 eV. We can conclude that the calculated small changes induced by increasing the number of Si atoms in the cluster make that comparisons between transitions calculated with clusters of different sizes remain sensible.

### 3. The side-on model

This di- $\sigma$  adsorption of the molecule on a site A, is simulated using a (single-dimer) Si<sub>9</sub>H<sub>12</sub> cluster. The optimized adsorption geometry is depicted in the inset of Fig. 10. In this cluster, which simulates four silicon (001) planes, all

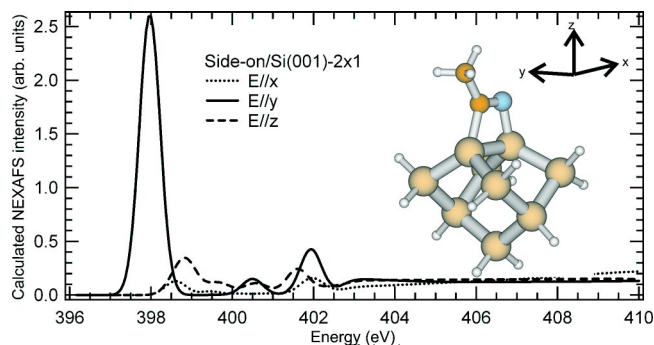


FIG. 10. (Color online) Calculated NEXAFS spectra of the side-on di- $\sigma$  cyclo-addition on site A, for three directions of the electric field. The optimized geometry is given in the inset.

atoms are allowed to relax. The Si<sub>2</sub> dimer is contained in the  $\mathbf{xz}$  plane. The CN distance is 1.29 Å (see Table II), a value expected for a C=N bond. Note that the resulting four-membered ring is strained, with  $\angle\text{SiCN}$  (109°) and  $\angle\text{CNSi}$  (103°) angles much smaller than the expected 120° for a  $sp^2$  hybridization. Therefore the Si-N axis makes an angle of about 13° with the normal to the surface ( $\mathbf{z}$ ).

The theoretical NEXAFS spectra are given in Fig. 10. The  $\pi_{\text{C}\equiv\text{N}}^*$  transition is calculated at  $h\nu=398$  eV. This transition is polarized in the  $\mathbf{y}$  direction (i.e., it vanishes in the  $\mathbf{x}$  and  $\mathbf{z}$  directions). Therefore, for a single-domain (vicinal) surface, the experimental absorption spectra of the side-on should exhibit strong dichroic effects. The absorption intensity should vanish at grazing incidence. At normal incidence it should strongly depend on the azimuthal direction of the field, i.e., maximum in the  $E_{\text{ortho}}$  geometry and zero in the  $E_{\text{para}}$  geometry (see Fig. 5). Another bound transition is found at 399 eV, polarized along the  $\mathbf{z}$  direction, i.e., the [001] direction. It corresponds to a " $\sigma_{\text{Si-N}}^*$ " the Si-N bond axis direction being close to that of the  $\mathbf{z}$  axis. The ionization potential (IP) is calculated at 403.26 eV.

### 4. The cumulative-double-bond (CDB) model

The CDB adsorption mode on site A, proposed by Mui *et al.*,<sup>12</sup> is simulated using a single-dimer cluster (Fig. 11 and Table II). The admolecule and the silicon dimer are contained in the  $\mathbf{xz}$  plane. The N=C=C axis makes an angle of 16° with  $\mathbf{z}$ . The N=C and C=C bond lengths are 1.21 Å and 1.31 Å, respectively.

We calculate a strong  $\pi^*$  transition at 399.3 eV, polarized along  $\mathbf{y}$  (i.e., in the  $\mathbf{xy}$  plane, perpendicularly to the dimer axis) followed by another  $\pi^*$  transition at 402.2 eV, polarized orthogonally to the preceding one. The calculated IP is 404.48 eV, 1.2 eV above that of the side-on.

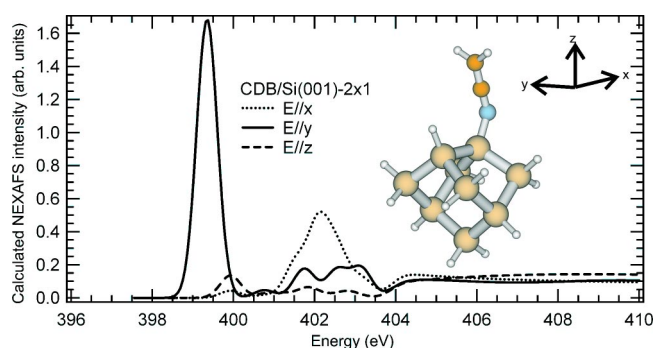


FIG. 11. (Color online) Calculated NEXAFS spectra of the dissociative adsorption mode, a cumulative double bond (CDB) and monohydride on site A, for three directions of the electric field. The optimized geometry is given in the inset.

### 5. The cyanomethyl models

The “free cyanomethyl plus silicon monohydride” geometry is calculated for a site A using a single-dimer cluster. The optimized geometry is represented in Fig. 12 (see also Table II for the geometrical outputs). The CN bond length is 1.16 Å, characteristic of a triple bond. As the other dissociated mode (the CDB plus Si-H mode), the cyanomethyl plus Si-H mode exhibits a larger adsorption heat than that of the nondissociated products (see Table I). The main  $\pi_{C\equiv N}^*$  is calculated at 399.9 eV. For  $E$  directed along  $x$  the absorption intensity is larger than along  $y$ , as a matter of fact, due to the electronic repulsion between the free cyano and the Si-H, the molecule rotates around its Si-C axis away from the  $xz$  plane (the dihedral angle  $\angle SiSiCC$  is  $57^\circ$ ). The calculated IP is 404.68 eV, 1.3 eV above that of the side-on.

Due to the almost free rotation around the Si-C bond, the cyanomethyl can make a dative bond with a neighboring silicon dangling bond of an adjacent dimer pertaining to the same row. The geometry of the datively bonded intrarow cyanomethyl is given in Fig. 13 (see also Table II). The CN bond length is 1.16 Å: as in the end-on case, the triple bond is not affected by the dative bonding. The  $\angle SiNC$  angle is  $125.4^\circ$ . In relation with this large Si-C $\equiv$ N bending—in the datively bonded end-on species, we calculate a  $\angle SiNC$  angle of about  $173^\circ$ —the  $\pi_{C\equiv N}^*$  transition splits into two contribu-

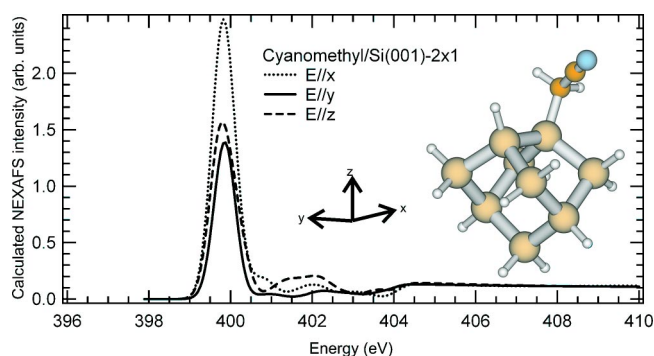


FIG. 12. (Color online) Calculated NEXAFS spectra of the dissociative mode, free-cyanomethyl and monohydride on site A, for three directions of the electric field. The optimized geometry is given in the inset.

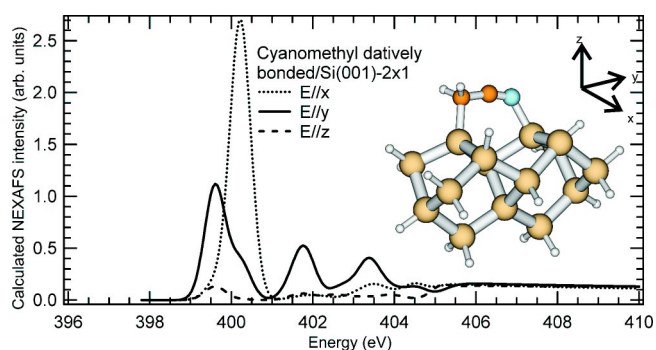


FIG. 13. (Color online) Calculated NEXAFS spectra of the dissociative mode, cyanomethyl datively bonded and monohydride on site B, for three directions of the electric field. The optimized geometry is given in the inset.

tions, the first one at 399.6 eV is polarized along  $z$  (grazing incidence), while the second one at 400.2 eV is polarized along  $y$  (normal incidence,  $E_{para}$  geometry). The calculated IP is 405.67 eV, 2.2 eV above that of the side-on.

### B. Simulation vs experiment and identification of the products

To help the discussion, the values of the calculated  $\pi^*$  transitions and IPs for the various models considered in Sec. V A are reported in Table III. The experimental data and their assignments are given in Table IV.

The calculations show that the (lowest  $h\nu$ ) NEXAFS transition measured at 387.8 eV and found strongly polarized in the surface plane (perpendicular to the dimer axis, i.e., in the  $E_{ortho}$  geometry) has the right energy transition and the right dichroism (*in the case of a single-domain surface*) to be attributed to a *side-on* species. However, we can notice, in the experimental spectrum (Fig. 6) of the vicinal surface, a residual  $\pi^*$  intensity along the dimer row direction ( $E_{ortho}$  geometry). This can be due to another adspecies di- $\sigma$  bonded at right angles with the side-on, i.e., the end bridge. Alternatively, this can arise from the formation of minority surface domains  $1 \times 2$ , rotated by  $90^\circ$  with respect to the  $2 \times 1$  terraces of the vicinal surface “staircase.” The dimension of the  $1 \times 2$  areas would be too small to be detected by LEED. In any case the side-on is the majority  $\pi_{C\equiv N}$  species (at saturation) after room temperature adsorption.<sup>31</sup> We attribute the XPS line found at a binding energy of  $\sim 397.8$  eV to this side-on species, which has indeed the lowest IP among all the calculated models (see Table III). (This gives an effective work function of  $\sim 5.5$  eV, that can be compared to the measured value of the clean surface, 4.9 eV.<sup>32</sup>)

On the one basis of its energy position, the NEXAFS transition measured at  $\sim 399$  eV could be attributed to the CDB model proposed by Mui *et al.*<sup>12</sup> (see Table II). However an examination of the NEXAFS transition polarizations eliminates the CDB model, indeed the calculation shows that the absorption intensity must be maximum at normal incidence, while, experimentally, it increases at grazing incidence (Figs. 6 and 7). For its part, the datively bonded cyanomethyl exhibits a calculated transition at 399.6 eV, with the right polarization (normal to the surface). However its IP

TABLE IV. Assignment of the experimental N 1s NEXAFS and XPS binding energies (given in eV) to adsorption models. FL represents Fermi level. CBM represents conduction band minimum.

| Experimental NEXAFS transitions | Experimental XPS binding energy respectively, to FL | Experimental XPS binding energy respectively, to CBM | Assigned model |
|---------------------------------|---|--|----------------|
| 397.8                           | 397.8   | 398.1±0.1  | Side-on        |
| 399                             | [N 1s <sup>FL</sup> (1)]                            | [N 1s <sup>CBM</sup> (1)]                            |                |
| 399.8                           | 398.7   | 399.0±0.1  | Free           |
|                                 | [N 1s <sup>FL</sup> (2)]                            | [N 1s <sup>CBM</sup> (2)]                            | Cyanomethyl    |

is 2.3 eV larger than that of the side-on. We do not see any structure in the N 1s XPS spectrum situated at a binding energy of ~400 eV, making the presence of this datively bonded cyanomethyl is unlikely.<sup>33</sup> The CDB and datively bonded cyanomethyl models cannot, therefore, account for the experimental line at 399 eV. In fact, the side-on model calculation provides a spectral line, the  $\sigma_{\text{Si-N}}^*$  transition, polarized normal to the surface and peaked at 398.8 eV (see Fig. 10), i.e., exhibiting the right energy and polarization.

The third experimental NEXAFS line at 399.8 eV is typical of a  $\pi_{\text{C}\equiv\text{N}}^*$  species, an end-on (calculated at 400.3 eV) or a free cyanomethyl (calculated at 399.9 eV). However the end-on has to be rejected because of its  $\pi_{\text{C}\equiv\text{N}}^*$  polarization in the surface plane and because of its large IP shift (3.5 eV) with respect to the side-on IP. For its part, the free cyanomethyl has a calculated NEXAFS transition at 399.9 eV and a calculated IP 1.3 eV higher in energy than that of the side-on. Therefore only the free cyanomethyl accounts both for the right  $\pi^*$  NEXAFS energy and for the measured binding energy shift of about 1 eV between the two N 1s XPS lines (Fig. 8). However we note that the calculated absorption intensity is dichroic in the *xy* plane [i.e., the (001) plane]. This is not observed experimentally for the single-domain surface (see Fig. 6). On the real surface, the molecule likely rotates around its Si-C axis at room temperature, averaging out the dichroic effects.

A general comment can be made on the present NEXAFS calculation. The agreement between the  $\Delta\text{KS}$  energy of the LUMO  $\pi^*$  transition and that obtained experimentally is striking. However our TP method fails to reproduce the step-like background observed experimentally for photon energies below IP (see Figs. 6 and 7). A step being attributed to transitions to substrate states mixed with molecular states,<sup>24</sup> its onset is expected at a photon energy equal to the N 1s binding energy measured from the silicon conduction band minimum (CBM). Therefore step onsets corresponding to the side-on and cyanomethyl species (see Table IV) are expected at ~398 eV[N 1s<sup>CBM</sup> (1)] and ~399 eV[N 1s<sup>CBM</sup> (2)], respectively.<sup>34</sup> Their positions are indicated in Fig. 7. As a matter of fact, we observe at  $h\nu \sim 399$  the onset of an intense step that the simulation of the cyanomethyl model (Fig. 12) does not reproduce. The reason for this discrepancy between theory and experiment results from the “molecular approach” we use here to calculate the transition intensities.

## VI. CONCLUSIVE REMARKS

N 1s NEXAFS/XPS data and DFT electronic transition calculations, have been used in combination to determine the

adsorption products of acetonitrile on Si(001) at 300 K. The calculation method; which has proven to be accurate for the isolated molecule, is applied to the case of adsorbates on surfaces, by simulating the semiconductor substrate by silicon clusters of various sizes. We have checked the influence of the cluster size on the transition energies in a particular case (the end-on adduct) and found that the effect is negligible for the NEXAFS transition and relatively small (within ~0.3 eV) for the IP energy.

Three main N 1s NEXAFS transitions are observed at 397.8 eV, 398.9 eV, and 399.8 eV. The NEXAFS transition energies and angular dependence, calculated for various models, allow the attribution of the three spectral lines to two geometries. One of the products results from a di- $\sigma$  bonding involving the cyano group, the experimental lines at 387.8 eV and 398.9 eV correspond to transitions to the  $\pi_{\text{C}\equiv\text{N}}^*$  orbital and  $\sigma_{\text{Si-N}}^*$  orbitals, respectively. The use of vicinal (single-domain) surfaces enables us to show that the “side-on” is the majority species of di- $\sigma$  type. Note that, on thermodynamic grounds, the paired end-bridge arrangement was found to be the most stable.<sup>11</sup> The third experimental line at 399.8 eV cannot be attributed to an end-on species (i.e., a datively bonded CH<sub>3</sub>CN) on the basis of calculated NEXAFS peak polarization and IP. It has to be attributed to a “free” C≡N moiety, a cyanomethyl moiety (Si-CH<sub>2</sub>-C≡N plus Si-H), not interacting with neighboring Si dangling bonds. The other possible dissociated product, the cumulative-double-bond (Si-N=C=CH<sub>2</sub> plus Si-H) proposed by Mui *et al.*,<sup>12</sup> exhibits calculated transitions at 399.3 eV (and 402.2 eV) but must be rejected on the basis of its NEXAFS angular dependence. Note that dissociation channels are blocked at 110 K, as only di- $\sigma$  adsorption modes are detected at this temperature.<sup>9</sup>

Besides the expected di- $\sigma$  adsorption mode, molecular dissociation occurs, due to the acidic nature of the  $\alpha$  hydrogen. However the observation of a cyanomethyl, instead of a cumulative-double-bond product, questions the pivotal role played by the end-on intermediate (Si-N≡C-CH<sub>3</sub>) in reaction paths calculations.<sup>12</sup> We recall that Miotto *et al.*<sup>13</sup> found that any attempt to “bend” the end-on leads to its desorption. Beyond this case study, the crucial role played by electron transition calculation to achieve a rigorous interpretation of the experimental NEXAFS/XPS data has also to be emphasized.

## ACKNOWLEDGMENTS

The authors are grateful for a generous allocation of computational time in the IBM RS/6000SP machine of IDRIS/CNRS.

- \*Also at Laboratoire pour l'Utilisation du Rayonnement Electromagnétique, Centre Universitaire Paris-Sud, Batiment 209D, 91405 Orsay Cedex, France. Electronic address: roch@ccr.jussieu.fr
- †Electronic address: carniato@ccr.jussieu.fr
- ‡Also at Université de Cergy-Pontoise, 95031 Cergy-Pontoise Cedex, France.
- <sup>1</sup>N. Guisinger, R. B. M. E. Greene, A. Baluch, and M. Hersam, *Nano Lett.* **4**, 55 (2004).
  - <sup>2</sup>M. Ono, A. Kamoshida, N. Matsuura, E. Ishikawa, T. Eguchi, and Y. Hasegawa, *Phys. Rev. B* **67**, 201306 (R) (2003).
  - <sup>3</sup>J. Shoemaker, L. W. Burggraf, and M. S. Gordon, *J. Chem. Phys.* **112**, 2994 (2000).
  - <sup>4</sup>Y. Jung, Y. Shao, M. S. Gordon, D. J. Doren, and M. Head-Gordon, *J. Chem. Phys.* **119**, 10917 (2003).
  - <sup>5</sup>R. Wolkow, *Annu. Rev. Phys. Chem.* **50**, 413 (1999).
  - <sup>6</sup>Q. Liu and R. Hoffmann, *J. Am. Chem. Soc.* **117**, 4082 (1995).
  - <sup>7</sup>H. Liu and R. Hamers, *J. Am. Chem. Soc.* **119**, 7593 (1997).
  - <sup>8</sup>In  $\text{CH}_3\text{-C}\equiv\text{N}$ , donation of a pseudo- $\pi$  orbital on the methyl group to the  $\pi$  orbital of the triple bond weakens the C-H bond. See P. M. Mayer, M. S. Taylor, M. W. Wong, and L. Radom, *J. Phys. Chem. A* **102**, 7074 (1998).
  - <sup>9</sup>F. Tao, Z. H. Wang, M. Qiao, Q. Liu, W. Sim, and G. Xu, *J. Chem. Phys.* **115**, 8563 (2001).
  - <sup>10</sup>F. Bournel, J.-J. Gallet, S. Kubsky, G. Dufour, F. Rochet, M. Simeoni, and F. Sirotti, *Surf. Sci.* **513**, 37 (2002).
  - <sup>11</sup>J. Cho and L. Kleinman, *J. Chem. Phys.* **119**, 6744 (2003).
  - <sup>12</sup>C. Mui, M. Fuller, S. F. Bent, and C. B. Musgrave, *J. Phys. Chem. B* **107**, 12256 (2003).
  - <sup>13</sup>R. Miotto, M. C. Oliveira, M. M. Pinto, F. de León-Pérez, and A. C. Ferraz, *Phys. Rev. B* **69**, 235331 (2004).
  - <sup>14</sup>J. H. Cho and L. Kleinman, *Phys. Rev. B* **69**, 075303 (2004).
  - <sup>15</sup>P. Mayer, M. S. Taylor, M. Wong, and L. Radom, *J. Phys. Chem. A* **102**, 7074 (1998).
  - <sup>16</sup>J. Stöhr, *NEXAFS Spectroscopy* (Springer, New York, 1992).
  - <sup>17</sup>L. Triguero, O. Plashkevych, L. G. M. Pettersson, and H. Agren, *J. Electron Spectrosc. Relat. Phenom.* **104**, 195 (1999).
  - <sup>18</sup>S. Carniato, V. Ilakovac, J.-J. Gallet, E. Kukk, and Y. Luo, *Phys. Rev. A* **70**, 032510 (2004).
  - <sup>19</sup><http://www.msg.ameslab.gov/GAMESS/GAMESS.html>
  - <sup>20</sup>Y. Widjaja and C. B. Musgrave, *Surf. Sci.* **469**, 9 (2000).
  - <sup>21</sup>A. Föhlisch, F. Hennies, W. Wurth, N. Witkowski, M. Nagasono, M. N. Piancastelli, L. V. Moskaleva, K. M. Neyman, and N. Rösch, *Phys. Rev. B* **69**, 153408 (2004).
  - <sup>22</sup>W. Kutzelnig, U. Fleisher, and M. Schindler, *Chemical Shifts and Magnetic Susceptibilities* (Springer-Verlag, New York, 1990), vol. 23.
  - <sup>23</sup>T. Ziegler, A. Rauk, and E. J. Baerends, *Theor. Chim. Acta* **43**, 261 (1977).
  - <sup>24</sup>J. Stöhr, *NEXAFS Spectroscopy* (Springer, New York, 1992), pp. 225–238.
  - <sup>25</sup>P. W. Langhoff, *Chem. Phys. Lett.* **22**, 60 (1973).
  - <sup>26</sup>A. Hitchcock, M. Tronc, and A. Modelli, *J. Phys. Chem.* **93**, 3068 (1989).
  - <sup>27</sup>D. Beach, C. Eyermann, S. Smit, S. Xiang, and W. Jolly, *J. Am. Chem. Soc.* **106**, 536 (1984).
  - <sup>28</sup>C. Mui, G. T. Wang, S. F. Bent, and C. B. Musgrave, *J. Chem. Phys.* **114**, 10170 (2001).
  - <sup>29</sup>X. Cao and R. Hamers, *J. Vac. Sci. Technol. B* **20**, 1614 (2002).
  - <sup>30</sup>S. Rangan, J.-J. Gallet, F. Bournel, S. Kubsky, K. Le Guen, G. Dufour, F. Rochet, F. Sirotti, S. Carniato, and V. Ilakovac, preceding paper, *Phys. Rev. B* **71**, 165318 (2005).
  - <sup>31</sup>We have calculated another  $\pi_{\text{C=N}}$  adsorption mode corresponding to a  $\text{Si-CH}_2\text{-HC=N-Si}$  moiety bridging the two dangling bonds of a silicon dimer (site A). This geometry is obtained after H transfer from the  $\alpha\text{C}$  to the next C atom. A five-membered ring results, much less strained than the four-membered ring of the side-on. The calculated NEXAFS spectrum gives a  $\pi_{\text{C=N}}^*$  transition at 398.2 eV and a  $\sigma_{\text{Si-N}}^*$  transition at 399.1 eV. The IP is calculated at 403.6 eV. Given that the NEXAFS and XPS signatures of this isomerized geometry are close to those of the side-on, STM and vibrational spectroscopy should be used to distinguish them. After adsorption at 110 K followed by annealing at 300 K a characteristic  $\text{CH}_3$  mode is observed with HREELS, eliminating this isomerized species (Ref. 9). However, vibrational spectra and STM images of acetonitrile directly adsorbed at room temperature have not been published yet.
  - <sup>32</sup>F. Himpsel, B. Meyerson, F. McFeely, J. Morar, A. Taleb-Ibrahimi, and J. Yarmoff, "Core level spectroscopy at silicon surfaces and interfaces," in *Proceedings of the Enrico Fermi School on Photoemission and Photoabsorption Spectroscopy of Solids and Interfaces with Synchrotron Radiation*, edited by M. Campagna and R. Rosei (North-Holland, Amsterdam, 1990), p. 203.
  - <sup>33</sup>The cyano group of a parent molecule, 3-butenenitrile ( $\text{H}_2\text{C=CH-CH}_2\text{-C}\equiv\text{N}$ ), apparently forms a dative bond with a silicon dangling bond, as a N 1s peak is measured at a binding energy of 399.9 eV [M. P. Schwartz and R. J. Hamers, *Surf. Sci.* **515**, 75 (2002)].
  - <sup>34</sup>The N 1s binding energy with respect to the conduction band minimum ( $\text{N } 1s^{\text{CBM}}$ ) is determined as follows. We have  $|\text{N } 1s\text{-CBM}| = |\text{N } 1s\text{-Si } 2p_{3/2}| + |\text{Si } 2p_{3/2}\text{-VBM}| + |\text{VBM-CBM}|$ , where VBM is the valence band maximum. The energy distance  $|\text{N } 1s\text{-Si } 2p_{3/2}|$  is measured experimentally,  $|\text{Si } 2p_{3/2}\text{-VBM}|$  is equal to 98.74 eV according to Himpsel *et al.* [F. J. Himpsel, G. Hollinger, and R. A. Pollak, *Phys. Rev. B* **28**, 7014 (1996)] or  $98.56 \pm 0.05$  eV, according to Ley *et al.* [L. Ley, J. Ristein, J. Schäfer, and S. Miyazaki *J. Vac. Sci. Technol. B* **14**, 3008 (1996)].  $|\text{VBM-CBM}|$  is the silicon band gap (1.12 eV).